Negative effective mass of wave-driven classical particles in dielectric media

A. I. Zhmoginov,* I. Y. Dodin,† and N. J. Fisch‡
Department of Astrophysical Sciences, Princeton Plasma Physics Laboratory, Princeton University, Princeton, New Jersey 08543, USA
(Received 12 October 2009; revised manuscript received 28 January 2010; published 11 March 2010)

For a classical particle undergoing nonlinear interaction with a wave in dielectric medium, a perturbation theory is developed, showing that the particle motion can be described in terms of an effective parallel mass which can become negative. A relativistic particle interacting with a circularly polarized wave and a static magnetic field is studied as an example. For the three stationary orbits corresponding to the same velocity parallel to the magnetic field, the conditions are found under which all these equilibria are centerlike, or neutrally stable. It is shown that a negative parallel mass is realized in the vicinity of the intermediate-energy equilibrium and can lead to a plasma collective instability.

DOI: 10.1103/PhysRevE.81.036404 PACS number(s): 52.35.Mw, 52.20.Dq, 52.27.Ny, 52.35.Qz

I. INTRODUCTION

The nonlinear resonance phenomenon, well understood for a one-dimensional (1D) oscillator [1–3], can exhibit intriguing and unexpected properties in other, yet still relatively simple physical systems. For instance, the presence of a nonlinear resonance at particle interaction with an oscillating field yields multiple branches of the ponderomotive potential [4]. On the other hand, it can also effectively modify the classical particle mass such that, for slow dynamics on time scales larger than the oscillation period, this mass is seen as negative [5]. (Further, we call this the "negative-mass effect," or NME.) Hence the possibility of effects similar to the absolute negative conductivity [6,7], the negative-mass instability [8–17], and related phenomena [18–20].

The conceptual possibility of NME was shown in Ref. [5] by considering a sample system such as a single particle in a static magnetic field and a circularly polarized "pump" wave in vacuum. In this particular case, the particle dynamics is exactly integrable, allowing one to derive NME from the least action principle directly [5]. However, of practical interest are wave interactions with particle ensembles (e.g., finite-density plasmas), in which case the wave dispersion differs from that in vacuum. As a rule, the corresponding particle trajectories cannot be found explicitly then, so the analytical approach used in Ref. [5] becomes virtually inapplicable. Thus, whether NME persists robustly in realistic environments remains to be studied.

In this paper, we develop a formalism, based on the Hamiltonian perturbation theory [21–23], that is suitable for treating general nonlinear interactions, albeit limited to sufficiently weak pump waves. We apply this formalism to study the particle effective mass and NME in a static magnetic field for an arbitrary refraction index n_0 of the pump wave (unlike in Ref. [5], limited to $n_0=1$). We show that the effective mass can become negative for n_0 within a nonzero interval and find the limitations on this interval depending on the wave parameters. Accordingly, the conditions are obtained under which a collective instability due to the modified mass can develop.

The paper is organized as follows. In Sec. II, we formulate the framework for our theory, starting off with a generalized Hamiltonian for a particle interacting with a wave. Particularly, we identify the stationary orbits and outline the approach to studying their stability. In Sec. III, we consider a charged particle interacting with a circularly polarized wave in the presence of a static background magnetic field. Based on the results of Sec. II, we find the stationary orbits for this problem and assess their stability. In Sec. III, we restate the parallel mass concept and calculate the parallel mass $m_\parallel$ for the problem of interest, showing when $m_\parallel$ can become negative. In Sec. IV, a plasma collective instability associated with $m_\parallel<0$ is introduced and the corresponding conditions are calculated. In Sec. V, we summarize our main conclusions.

II. GENERALIZED WAVE-PARTICLE INTERACTION

Consider a general system governed by a Hamiltonian of the form

$$H = H_0(\boldsymbol{I}) + \varepsilon H_1(\boldsymbol{I})\cos(\boldsymbol{\ell}\cdot\boldsymbol{\phi} - \omega t), \tag{1}$$

where H_0 is the Hamiltonian of the unperturbed system, H_1 is the perturbation Hamiltonian describing the particle interaction with a wave [22], $\varepsilon \ll 1$ is a small parameter, $\boldsymbol{I}$ is the n-dimensional action vector, $\boldsymbol{\phi}$ is the conjugate angle vector, and $\boldsymbol{\ell}=(\ell_1,\ldots,\ell_n)$ is some constant integer vector. (Both H_0 and H_1 can also slowly depend on time t, but, since this dependence does not affect our considerations, we will omit it from our equations for brevity.) Without loss of generality, assume nonzero ℓ_n. Then, performing a canonical transformation to the new actions $\boldsymbol{J}$ and the new angles $\boldsymbol{\theta}$ via the generating function $\Phi(\boldsymbol{J},\boldsymbol{\phi},t)=\phi_1 J_1+\cdots+\phi_{n-1}J_{n-1}+(\boldsymbol{\ell}\cdot\boldsymbol{\phi}-\omega t)J_n$, one can write the new Hamiltonian $\mathcal{H}\equiv H+\partial\Phi/\partial t$ as

$$\mathcal{H} = H_0(\boldsymbol{I}) - \omega J_n + \varepsilon H_1(\boldsymbol{I})\cos\,\theta_n, \tag{2}$$

where

$$J_i = I_i - \ell_i I_n/\ell_n \quad (i<n), \tag{3}$$

*azhmogin@princeton.edu
†idodin@princeton.edu
‡fisch@princeton.edu

$$J_n = I_n/\ell_n. \tag{4}$$

Since $\mathcal{H}$ is independent of the $n-1$ new angles $\theta_i=\phi_i$ for $i<n$, the corresponding new actions J_i are conserved. Therefore, the perturbed system is integrable and can be described by just two equations,

$$\dot{J}_n = \varepsilon H_1(\boldsymbol{I})\sin\,\theta_n, \tag{5}$$

$$\dot{\theta}_n = \omega_n(\boldsymbol{I}) - \omega + \varepsilon\Omega_n(\boldsymbol{I})\cos\,\theta_n, \tag{6}$$

where $\omega_n(\boldsymbol{I})=\boldsymbol{\ell}\cdot\partial H_0/\partial\boldsymbol{I}$ and $\Omega_n(\boldsymbol{I})=\boldsymbol{\ell}\cdot\partial H_1/\partial\boldsymbol{I}$.

The dynamics of the system described by Eqs. (5) and (6) is determined by the types of its stationary points in (θ_n,J_n) plane (or, more precisely, cylinder), which are found from

$$\dot{J}_n = 0, \quad \dot{\theta}_n = 0. \tag{7}$$

Those include

$$\omega_n(\boldsymbol{I}) - \omega + \varepsilon\Omega_n(\boldsymbol{I}) = 0, \quad \theta_n = 0, \tag{8}$$

$$\omega_n(\boldsymbol{I}) - \omega - \varepsilon\Omega_n(\boldsymbol{I}) = 0, \quad \theta_n = \pi, \tag{9}$$

and an additional family of stationary points found from

$$H_1(\boldsymbol{I}) = 0, \quad \omega_n(\boldsymbol{I}) - \omega + \varepsilon\Omega_n(\boldsymbol{I})\cos\,\theta_n = 0. \tag{10}$$

In $\boldsymbol{J}$ space, the stationary points given by Eqs. (8)–(10) form a set of $(n-1)$-dimensional manifolds, which we will further call stationary surfaces (or stationary curves, if $n=2$).

The stability of the stationary solutions with respect to small perturbations is determined by the eigenvalues $\boldsymbol{\lambda}$ of the Jacobian matrix calculated for the linearized Eqs. (5) and (6) in the vicinity of each stationary point s with $\boldsymbol{J}=\boldsymbol{J}^s$ and $\theta_n=\theta_n^s$. For the equilibrium described by Eqs. (8) and (9), one has

$$\lambda_{1,2}^2 = \varepsilon H_1\boldsymbol{\ell}\cdot\left(\left.\frac{\partial\omega_n}{\partial\boldsymbol{I}}\right|_s + \varepsilon\left.\frac{\partial\Omega_n}{\partial\boldsymbol{I}}\right|_s\cos\,\theta_n^s\right)\cos\,\theta_n^s, \tag{11}$$

whereas for the other type of stationary points, described by Eq. (10), one has

$$\lambda_1 = \varepsilon\Omega_n(\boldsymbol{J}^s)\sin\,\theta_n^s, \tag{12}$$

$$\lambda_2 = -\varepsilon\Omega_n(\boldsymbol{J}^s)\sin\,\theta_n^s. \tag{13}$$

Since Eqs. (12) and (13) yield $\lambda_1+\lambda_2=0$, the equilibrium solving $H_1=0$ always corresponds to a saddle. Of primary interest, however, are centerlike equilibria, which can hold particles on larger time scales. Such stable points are only possible via Eq. (11), and if $\lambda_{1,2}^2<0$. The manifolds formed in $\boldsymbol{J}$ space by these points will be called stable surfaces.

Any point on any connected stable surface can be transformed into any other point on this surface, by applying additional forces, assuming that they are sufficiently weak (so the surface itself persists) and slow (so the perturbation is adiabatic). To illustrate this, consider a system described by the Hamiltonian (1) yet with an additional term of the form $-\boldsymbol{f}(t)\cdot\boldsymbol{\phi}$. In this case, the stationary points of Eqs. (5) and (6) are not perturbed significantly, and the adiabatic invariant $\oint J_n d\theta_n$ associated with the rapid oscillations in (θ_n,J_n) space is conserved. Therefore, a particle located near the stable surface $J_n(J_1,\ldots,J_{n-1})$ will remain in its vicinity, even if the overall displacement in $\boldsymbol{J}$ space is substantial. The displacement itself is governed by $\dot{J}_i=g_i$, where $g_i=f_i-\ell_i f_n/\ell_n$ for $i<n$. However, in the original $\boldsymbol{I}$ space, the drift equations for the particle moving along the stable surface have an additional term, which originates from Eq. (3):

$$\dot{I}_i = g_i + l_i\sum_{k=1}^{n-1} g_k\frac{\partial J_n}{\partial J_k}. \tag{14}$$

Such a response to the external force is different from that of a system not subjected to the weak perturbation H_1.

In application to the wave-particle interaction problem, discussed in the following sections, this means that the response of an "oscillating" particle to an external force F can be different from that of a particle which is at rest or undergoes slow motion only. Specifically, an *effective mass* can be assigned to the particle [5,24], according to

$$m_\parallel\dot{v} = F. \tag{15}$$

For simplicity, we only consider 1D dynamics here; hence the index $\parallel$, reflecting that v is assumed parallel to F. In the sections to follow, we show that $m_\parallel$ can be very different from the particle rest mass m, even for weakly relativistic oscillations; thus, properties of "metaplasma" composed of such oscillation centers can be different from those of "normal" plasmas.

III. MAGNETIZED PARTICLE IN A WAVE

A. Basic equations

A significant effect on the particle parallel mass can be caused, for example, by a sufficiently strong electromagnetic wave propagating close to the nonlinear cyclotron resonance with a charged particle in a static magnetic field. To see this, assume homogeneous magnetic field of the form $\boldsymbol{B}_0=B_0\hat{\boldsymbol{z}}$, governed by the vector potential $\boldsymbol{A}_0=-\hat{\boldsymbol{x}}By$, and the "pump" wave field with circular polarization, governed by $\boldsymbol{A}_w=(mc^2/q)(a_0/\sqrt{2})(\hat{\boldsymbol{x}}\cos\,\xi-\hat{\boldsymbol{y}}\sin\,\xi)$, where m and q are the particle mass and charge correspondingly, c is the speed of light, a_0 is the normalized wave field amplitude, $\hat{\boldsymbol{x}}$, $\hat{\boldsymbol{y}}$, and $\hat{\boldsymbol{z}}$ are unit vectors directed along x, y, and z correspondingly, and $\xi=\omega t-kz$. The particle Hamiltonian reads as

$$H = \sqrt{m^2c^4 + c^2(\boldsymbol{P}-q\boldsymbol{A}/c)^2}, \tag{16}$$

where $\boldsymbol{A}=\boldsymbol{A}_0+\boldsymbol{A}_w$, and $\boldsymbol{P}$ is the particle canonical momentum. We assume that the wave field is weak and hence treat $\boldsymbol{A}_w$ as a perturbation. Therefore, after a canonical transformation to the new actions

$$\tilde{\mu} = (\boldsymbol{P}-q\boldsymbol{A}_0/c)^2/(2m\Omega_0), \quad m\Omega_0 X = m\Omega_0 x + P_y \tag{17}$$

and the new angle variables

$$\tilde{\theta} = \tan^{-1}[(P_x+m\Omega_0 y)/P_y] + \pi/2, \quad Y = -P_x/(m\Omega_0), \tag{18}$$

similarly to Ref. [23], $H\approx H_0+\varepsilon H_1\cos(\tilde{\theta}-\omega t+kz)$ can be approximated as

$$H = H_0 - \frac{\varepsilon \tilde{\mu}^{1/2}}{H_0}\cos(\tilde{\theta} - \omega t + kz), \tag{19}$$

where $H_0 = c(m^2c^2 + 2m\Omega_0\tilde{\mu} + p_\parallel^2)^{1/2}$ is the particle Hamiltonian without the wave, $p_\parallel \equiv P_z$ is the component of the kinetic momentum parallel to $\boldsymbol{B}_0$, $\varepsilon = mc^3\sqrt{m\Omega_0 a_0}$ is the normalized amplitude playing the role of the small parameter, $\Omega_0 = qB_0/mc$ is the nonrelativistic Larmor frequency, and $\tilde{\mu}$ is the canonical momentum, which is related to the particle magnetic moment $\mu \equiv p_\perp^2/(2m\Omega_0)$ (here $\boldsymbol{p}_\perp$ is the kinetic momentum transverse to $\boldsymbol{B}_0$) as

$$\mu = \tilde{\mu} + \frac{mc^2 a_0^2}{4\Omega_0} - a_0 c\sqrt{\frac{m\tilde{\mu}}{\Omega_0}}\cos(\tilde{\theta} - \omega t + kz). \tag{20}$$

[Note that, unlike in Eq. (2), the small parameter ε is dimensional here.]

Following the general formalism of Sec. II, we introduce the action and the angle variables of the unperturbed problem

$$I_1 = p_\parallel/k, \quad \phi_1 = kz, \tag{21}$$

$$I_2 = \tilde{\mu}, \quad \phi_2 = \tilde{\theta}. \tag{22}$$

Representing $\tilde{\theta} - \omega t + kz$ as $\boldsymbol{\ell}\cdot\boldsymbol{\phi} - \omega t$, where $\boldsymbol{\ell} = (1,1)$, we obtain then

$$J_1 = p_\parallel/k - \tilde{\mu}, \quad \theta_1 = kz, \tag{23}$$

$$J_2 = \tilde{\mu}, \quad \theta_2 = \tilde{\theta} - \omega t + kz. \tag{24}$$

Hence, we put Eq. (19) in the form (2), now reading as

$$\mathcal{H} = H_0 - \omega J_2 - \frac{\varepsilon\sqrt{J_2}}{H_0}\cos\,\theta_2, \tag{25}$$

where

$$H_0 = c[m^2c^2 + 2m\Omega_0 J_2 + k^2(J_1 + J_2)^2]^{1/2}. \tag{26}$$

In the sections to follow, we discuss the stationary points of the Hamiltonian (25) and their stability, showing that unexpected dynamics can result in this seemingly well-studied problem.

B. Stationary curves

The stationary points of the system governed by the Hamiltonian (25) form two different families. The first one is comprised of those solving $H_1(J_1, J_2) = 0$ and $\cos\,\theta_2 = 0$ (simultaneously), which corresponds to, respectively,

$$\tilde{\mu} = 0, \quad \theta_2 = \pi/2, \tag{27}$$

$$\tilde{\mu} = 0, \quad \theta_2 = 3\pi/2. \tag{28}$$

The second family, which we will focus on, is obtained by solving Eqs. (8) and (9):

$$\frac{\Omega_0}{\tilde{\gamma}} + \frac{kp_\parallel}{m\tilde{\gamma}} - \omega + \varepsilon Q = 0, \quad \theta_2 = 0, \tag{29}$$

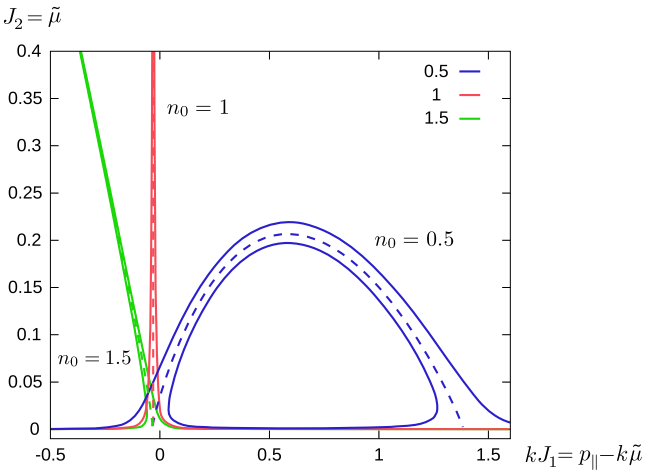

FIG. 1. (Color online) Stationary curves solving Eqs. (29) and (30) for $\varepsilon = 0$ (dashed) and $\varepsilon = 0.01$ (solid) for $n_0 = 0.5, 1, 1.5$ and $\omega = 0.97\Omega_0$ (in units $m = q = c = 1$).

$$\frac{\Omega_0}{\tilde{\gamma}} + \frac{kp_\parallel}{m\tilde{\gamma}} - \omega - \varepsilon Q = 0, \quad \theta_2 = \pi, \tag{30}$$

where we introduced

$$Q = \frac{m^2c^2 + p_\parallel^2 - 2kp_\parallel\tilde{\mu}}{2m^3c^4\tilde{\gamma}^3\sqrt{\tilde{\mu}}}, \tag{31}$$

and $\tilde{\gamma} \equiv H_0/mc^2$ is the Lorentz factor of the unperturbed motion.

The shape of the stationary curves can be established for sufficiently small ε by neglecting the terms proportional to ε in Eqs. (29) and (30). Substituting $\varepsilon = 0$ in these equations, one obtains two asymptotic zeroth-order solutions,

$$\tilde{\mu} = 0, \tag{32}$$

$$\tilde{\mu} = \frac{(n_0^2 - 1)p_\parallel^2}{2m\Omega_0} + \frac{n_0 c p_\parallel}{\omega} + \frac{mc^2}{2\Omega_0}\left(\frac{\Omega_0^2}{\omega^2} - 1\right), \tag{33}$$

where $n_0 \equiv ck/\omega$ is the medium refraction index. In variables $(p_\parallel, \tilde{\mu})$, Eq. (33) describes a parabola, concave for $n_0 < 1$ and convex for $n_0 > 1$. (One can show, however, that, in the latter case, only one of the branches of this parabola is physically realizable.) In (J_1, J_2) space, Eq. (33) is rewritten as

$$\frac{\Omega_0^2}{\omega^2} - 1 + \frac{n_0^2\omega^2(J_1 + J_2)^2(n_0^2 - 1)}{m^2c^4} + \frac{2\Omega_0[n_0^2 J_1 + (n_0^2 - 1)J_2]}{mc^2} = 0, \tag{34}$$

which can be shown to yield a single-valued dependence $J_2(J_1)$ (dashed curves in Fig. 1) in the upper half plane $J_2 \geq 0$.

For nonzero ε, multivalued dependence is realized (solid curves in Fig. 1), which can be seen as follows. Rewrite Eqs. (29) and (30) as $\Lambda(\tilde{\mu}, p_\parallel) = \pm\varepsilon$ where $\Lambda = (\Omega_0 + kp_\parallel/m - \omega\tilde{\gamma})/(\tilde{\gamma}Q)$ is the normalized detuning from the (Doppler-shifted) cyclotron resonance. Since the derivative $\partial\Lambda/\partial\tilde{\mu}$

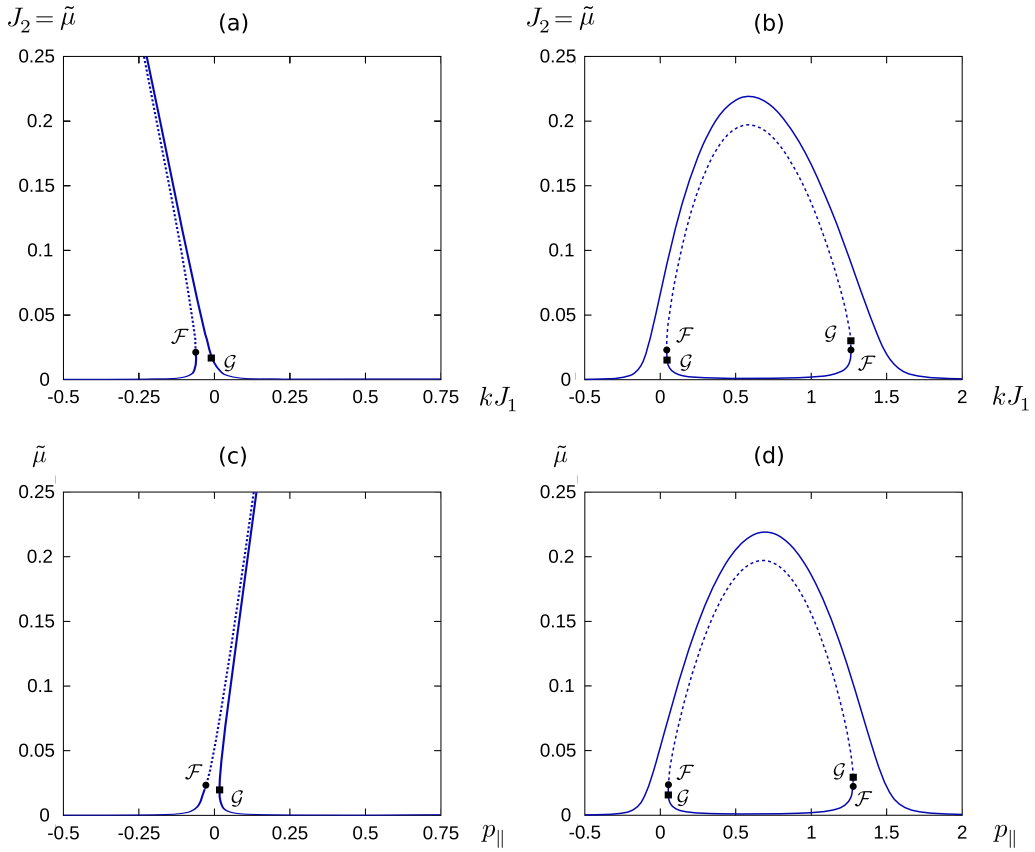

FIG. 2. (Color online) Stationary curves plotted for the same parameters as in Fig. 1 for $n_0=1.5$ [(a) and (c)] and $n_0=0.5$ [(b) and (d)] in coordinates $(kJ_1, J_2=\tilde{\mu})$ [(a) and (b)] and in coordinates $(p_\parallel, \tilde{\mu})$ [(c) and (d)]. Unstable branches (dashed) lie above the critical points (dots), at which dJ_2/dJ_1 is infinite. Stable branches (solid) are those below the critical points and also those corresponding to single-valued $J_2(J_1)$. Here $\mathcal{F}=(J_1^*, J_2^*)$ is the critical point where dJ_2/dJ_1 is infinite; $\mathcal{G}$ is the critical point where $d\tilde{\mu}/dp_\parallel$ is infinite; $J_1=p_\parallel/k-\tilde{\mu}$, $J_2=\tilde{\mu}$.

does not generally vanish on the curve given by Eq. (33) and since $\Lambda(\tilde{\mu}, p_\parallel) \sim \sqrt{\tilde{\mu}}$, assuming that $p_\parallel$ avoids the vicinities of the zeroes of Eq. (33), one can show that there will be a single perturbed solution $\tilde{\mu}$ corresponding to the unperturbed solution (32) and two perturbed solutions corresponding to Eq. (33). The same property holds for the stationary curves in (J_1, J_2) space. Therefore, depending on $p_\parallel$ (or J_1) there are either one, or three solutions $\tilde{\mu}$ (or J_2) of Eqs. (29) and (30).

The bifurcation, or critical points $\mathcal{F}$ are the points, at which the transition between one and three solutions in (J_1, J_2) plane occurs (Fig. 2). The critical point, which becomes weakly relativistic for $n_0 \approx 1$ and $\omega \approx \Omega_0$ as ε goes to zero, can be found as follows. Multiply Eqs. (29) and (30) by $\tilde{\gamma}\sqrt{J_2}$ to rewrite them as

$$\sqrt{J_2} F_0(J_1, J_2, \chi) \pm \varepsilon F_1(J_1, J_2, \chi) = 0, \tag{35}$$

where $\chi \equiv n_0 - 1$,

$$F_0 = \Omega_0 + \frac{kp_\parallel}{m} - \omega\tilde{\gamma}, \quad F_1 = \tilde{\gamma} Q \sqrt{J_2}. \tag{36}$$

Assuming $\chi \ll 1$, we solve Eq. (35) perturbatively in both ε and χ. To do so, consider first the unperturbed solution corresponding to $\varepsilon=0$ and $\chi=0$,

$$J_1 = J_1^0 = \frac{mc^2(\omega^2 - \Omega_0^2)}{2\omega^2\Omega_0}. \tag{37}$$

Hence, the perturbation $\delta J_1(J_2)$ can be expressed as

$$\delta J_1 \approx -\chi \frac{\partial F_0/\partial\chi}{\partial F_0/\partial J_1} - \frac{\varepsilon F_1}{\sqrt{J_2}\,\partial F_0/\partial J_1}, \tag{38}$$

where the derivatives of F_0 are taken at $J_1=J_1^0$ and $\chi=0$. Substituting the expressions for F_0 and F_1 in Eq. (38), one finally obtains

$$\delta J_1 = -\frac{\sqrt{J_2}(\varepsilon + 2J_2^{3/2}\chi\omega^2)}{2mc^2\Omega_0} + \frac{(1+\Omega_0^2/\omega^2)(\varepsilon - 4J_2^{3/2}\chi\omega^2)}{4\sqrt{J_2}\Omega_0^2} - \frac{mc^2\chi(\omega^2/\Omega_0^2 + 2 - 3\Omega_0^2/\omega^2)}{4\Omega_0}. \tag{39}$$

A tedious yet straightforward calculation yields that the critical point $\mathcal{F}=(J_1^*, J_2^*)$, where $d(\delta J_1)/dJ_2$ vanishes, is given by $J_1^*=J_1^0+\delta J_1(J_2^*)$,

$$J_2^* = \left(\frac{\varepsilon}{8|\chi|\omega^2}\right)^{2/3}, \tag{40}$$

and resides within the validity domain of the perturbation theory developed here for small ε and χ. In other words,

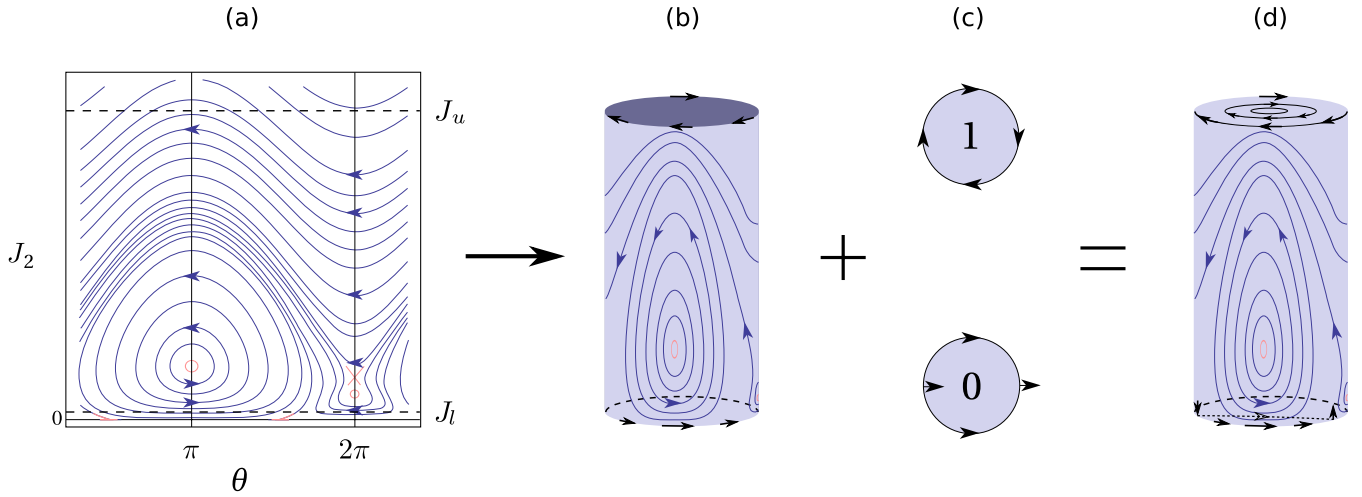

FIG. 3. (Color online) Construction of a compact manifold with a continuous vector field from a part ($\hat{J}_l < J_2 < \hat{J}_u$) of the original Hamiltonian vector field defined for $J_2 > 0$ (a). The latter is considered on a cylinder (b) to which we add two "caps," one at the top and one at the bottom (c). Using the asymptotic behavior of the original field at large and small J_2, the vector field is continued analytically to the caps, resulting in the upper cap Poincaré index $\zeta_u = 1$ and the lower cap index $\zeta_l = 0$, assuming n_0 is not equal to unity. The resulting manifold (d) is compact; hence, the Poincaré-Hopf theorem can be applied, allowing to formally deduce the stability of the equilibria on the plot (a) without calculating the corresponding eigenvalues $\boldsymbol{\lambda}$, otherwise found from Eqs. (11)–(13).

infinite dJ_2/dJ_1 corresponds to $\tilde{\mu} = \mu_*$, where

$$\mu_*^{3/2} = \left(\frac{mc^2}{\omega}\right)^{3/2} \frac{a_0}{8|1-n_0|} \sqrt{\frac{\Omega_0}{\omega}}. \tag{41}$$

C. Stability of the stationary points

By definition, each of the points on the stationary curves $J_1(J_2)$ found in Sec. III B, corresponds to a stationary orbit with fixed actions J_1 and J_2 (or, alternatively, fixed $\tilde{\mu}$ and $p_\parallel$). While those corresponding to $H_1(J_2) = 0$ are always saddles (Sec. II), the stability of the stationary trajectories corresponding to $\theta_2 = 0$ and $\theta_2 = \pi$ may vary and can be assessed as follows.

The Hamiltonian flow on the phase cylinder (θ_2, J_2) can exhibit only two types of equilibria, namely, centers which are stable stationary points with Poincaré index $\zeta = 1$, and saddles, which are unstable points with index $\zeta = -1$ [25,26]. It turns out that, for the Hamiltonian (19), this fact is sufficient to predict the type of stationary points without calculating the eigenvalues $\boldsymbol{\lambda}$. Specifically, one can do this by using the Poincaré-Hopf theorem [25–27], for which to be applicable we will need to transform the phase cylinder into a compact orientable differentiable manifold. The latter is done as follows.

Using the asymptotic expansions of H_0 and H_1 and their derivatives near $J_2 = 0$ and at $J_2 \to \infty$, choose some $\hat{J}_l$ and $\hat{J}_u > \hat{J}_l$ for which the Hamiltonian vector field governed by Eq. (19) is continued smoothly to the cylinder "caps" at $J_2 = \hat{J}_l$ and $J_2 = \hat{J}_u$ (Fig. 3). Specifically, assuming that $\omega \sim \Omega_0$, choose $\hat{J}_u$ such that $\hat{J}_u \gg J_1$, $\hat{J}_u \gg mc^2/\Omega_0$, and $\hat{J}_u^{3/2} \gg \varepsilon(2n_0|\chi|\omega^2)^{-1}$. In this case, the Hamiltonian equations following from Eq. (19) can be approximated by

$$\dot{J}_2 \approx -\varepsilon(n_0^2\omega^2\hat{J}_u)^{-1/2}\sin\theta_2, \tag{42}$$

$$\dot{\theta}_2 \approx \omega(n_0 - 1) + \varepsilon(2n_0\omega\hat{J}_u^{3/2})^{-1}\cos\theta_2. \tag{43}$$

Hence, the flow on the upper rim of the cylinder is as shown in Fig. 3(b), meaning that the cap has the index $\zeta_u = 1$ [Fig. 3(c)].

Similarly, consider the vicinity of $J_2 = 0$. For $\hat{J}_l \ll mc^2/\Omega_0$, the canonical equations read as

$$\dot{J}_2 \approx -\varepsilon\hat{J}_l^{1/2}(m^2c^4 + n_0^2\omega^2J_1^2)^{-1/2}\sin\theta_2, \tag{44}$$

$$\dot{\theta}_2 \approx -\varepsilon(4\hat{J}_l)^{-1/2}(m^2c^4 + n_0^2\omega^2J_1^2)^{-1/2}\cos\theta_2. \tag{45}$$

Hence, the flow on the lower rim is different from that on the upper rim [Fig. 3(b)], yielding the index $\zeta_l = 0$.

The cylinder considered together with the two caps forms a compact manifold [Fig. 3(d)] diffeomorphic to a sphere, to which the Poincaré-Hopf theorem can be applied. Specifically, the latter states that all the equilibrium indexes on the manifold sum up to 2. Subtracting the contribution from the caps ($\zeta_u + \zeta_l = 1$), one gets

$$\sum_s \zeta_s = 1, \tag{46}$$

for the stationary points with $J_2 > 0$ on the original cylinder without the caps. Recall now that there exist either one or three solutions for a stationary point at nonzero J_2 (Sec. III B; having two solutions is the intermediate degenerate case). In the former case, Eq. (46) yields that the only equilibrium is a center, whereas in the latter case there must exist two centers and one saddle [30].

It now remains to figure out *which* of the points corresponds to the saddle. Since the latter appears only when $J_2(J_1)$ becomes double-valued at one of the branches (as we

just showed), consider a pair of equilibria corresponding to the double-valued $J_2(J_1)$ at fixed J_1 (Fig. 2). The related eigenvalues $\boldsymbol{\lambda}$ are given by

$$\lambda^2 = \varepsilon H_1 \frac{dR}{dJ_2}\cos\,\theta_2, \tag{47}$$

where $R(J_2)=\omega_n(J_2)-\omega+\varepsilon\Omega_0(J_2)\cos\,\theta_2$ is such that it equals zero at each of the equilibria. Due to the latter, dR/dJ_2 must have different signs at the two stationary points corresponding to a given J_1 and θ_2. And since $H_1>0$, the sign of λ^2 has to be different in these points as well. Therefore, the saddle *always* corresponds to one of the branches of the double-valued $J_2(J_1)$. Since at $\chi\to 0$ the critical point $\mathcal{F}$, which separates the two branches, goes to infinity, we further conclude that it must be the intermediate branch that is unstable [Figs. 2(a) and 2(b)].

D. Tristability

Now consider the same stationary curves in coordinates $(p_\parallel,\tilde{\mu})$ [Figs. 2(c) and 2(d)]. In this case, the curves look similar to those in coordinates (J_1,J_2) [Figs. 2(a) and 2(b)] in that they also exhibit a bifurcation point (one or two), further called $\mathcal{G}$, where $d\tilde{\mu}/dp_\parallel$ is infinite. As follows from Eq. (23), this new point $\mathcal{G}$ corresponds to $dJ_2/dJ_1=-1$, and therefore does *not* map to the bifurcation point $\mathcal{F}$ (corresponding to infinite dJ_2/dJ_1), where the stability is lost (Sec. III C). Particularly, for $n_0>1$, $\mathcal{G}$ falls below $\mathcal{F}$, i.e., into the interior of the stability region, whereas for $n_0<1$, there are two points $\mathcal{G}$, exactly one of which falls into the stability region. Hence, in either case, there can be up to three different *stable* stationary points for a given $p_\parallel$.

In other words, unlike a "normal" 1D nonlinear oscillator undergoing near-resonant interaction with an external force, where only up to two stable stationary orbits are possible [1,2], a wave-driven particle in a magnetic field is *tristable*. Previously, this tristability was demonstrated for the degenerate case $n_0=1$, by exact integration of the particle motion equation [5]. The perturbative analysis offered above shows that the tristability is a robust effect, also holding for n_0 other than unity, and therefore could be observed in real physical systems. In what follows, we show that this effect yields important implications regarding the particle response to fields *additional* to $\boldsymbol{B}_0$ and the wave; particularly, negative $m_\parallel$ can result.

E. Effective parallel mass

Suppose an additional low-frequency perturbation force F along z, so the Hamiltonian (25) can be written as

$$\mathcal{H} = H_0 - \omega J_2 - \frac{\varepsilon\sqrt{J_2}}{H_0}\cos\,\theta_2 - F\theta_1/k, \tag{48}$$

where we used that $z=\theta_1/k$ [Eq. (23)]. Due to the oscillations in the high-frequency field and the static magnetic field, the particle mass is effectively modified, yielding that the parallel mass

$$m_\parallel \equiv F/\dot{v}, \tag{49}$$

which can further be rewritten as

$$m_\parallel \approx mF\left[\frac{d}{dt}\left(\frac{p_\parallel}{\tilde{\gamma}}\right)\right]^{-1}, \tag{50}$$

no longer equals the rest mass m (Sec. II). By analogy with the particle dynamics in a crystal [29], the particle motion along z corresponding to Eq. (48), can then be described by the Hamiltonian

$$H_{\text{eff}}(p,z) = K(p) + U(z). \tag{51}$$

Here $U(z)$ is the potential energy satisfying $F=-U'(z)$; $K(p)$ is the effective kinetic energy, or "quasienergy," related to $m_\parallel$ through

$$m_\parallel^{-1} = d^2K/dp^2; \tag{52}$$

and p is the canonical momentum, or the "quasimomentum," related to $v\equiv\dot{z}$ through $v=dK/dp$ (see also Sec. IV). Since $\dot{p}=k\dot{J}_1=F$, one has $p=kJ_1$, not to be confused with $p_\parallel$.

Using Eqs. (23) and (26) to represent $p_\parallel$ and $\tilde{\gamma}$ as functions of J_1 and J_2, Eq. (50) can be written as

$$\frac{m_\parallel}{m} = F\left[\frac{d}{dt}\left(\sqrt{\frac{m^2c^2k^2(J_1+J_2)^2}{m^2c^2+2m\Omega_0J_2+k^2(J_1+J_2)^2}}\right)\right]^{-1}. \tag{53}$$

From Eq. (48), one has $\dot{J}_1=F/k$. To find $\dot{J}_2$, for simplicity, suppose a particle in the vicinity of a stationary state and recall (Sec. II) that it will remain in this vicinity as long as the perturbation force F is adiabatic. As the stationary state itself evolves in response to F, the particle will follow the stationary curve $J_2(J_1)$; thus,

$$\dot{J}_2 = (dJ_2/dJ_1)\dot{J}_1. \tag{54}$$

Using these, we now rewrite Eq. (53) as

$$\frac{m_\parallel}{m} = \left[\frac{1+dJ_2/dJ_1}{\tilde{\gamma}}\left(1-\frac{p_\parallel}{\tilde{\gamma}}\frac{\partial\tilde{\gamma}}{\partial p_\parallel}\right) - \frac{p_\parallel}{k\tilde{\gamma}^2}\frac{\partial\tilde{\gamma}}{\partial\tilde{\mu}}\frac{dJ_2}{dJ_1}\right]^{-1}. \tag{55}$$

After simplification, one finally obtains

$$m_\parallel = m\tilde{\gamma}^3\left[1+\frac{2\tilde{\mu}\Omega_0}{mc^2}+\left(1-\frac{p_\parallel\Omega_0}{mc^2k}+\frac{2\tilde{\mu}\Omega_0}{mc^2}\right)\frac{dJ_2}{dJ_1}\right]^{-1}. \tag{56}$$

As seen in Fig. 4, Eq. (56) agrees with the results of Ref. [5], where a different derivation for $m_\parallel$ was proposed, limited to $n_0=1$.

From Fig. 4 (and Ref. [5]), one can conclude that $m_\parallel$ exhibits multiple branches and *can* become negative; we now explore more generally *when* this happens. The sign of $m_\parallel$ changes where $m_\parallel$ becomes zero or infinite. The first case is realized when $dJ_1/dJ_2=0$, which is exactly the bifurcation point $\mathcal{F}$ (Sec. III B). The second one corresponds to the zero of the denominator in Eq. (56). Assuming that the particle is weakly relativistic, or $p_\parallel\ll mc$ and $\tilde{\mu}\ll mc^2/\Omega_0$, one concludes that $dJ_2/dJ_1\approx -1$. Therefore, $m_\parallel$ is singular at the point $\mathcal{G}'$, which is close to the point $\mathcal{G}$, where $d\tilde{\mu}/dp_\parallel$ is infinite. Hence, the negative-mass region is located on the stationary curves between the points with zero and infinite $m_\parallel$, corresponding to $\mathcal{F}$ and $\mathcal{G}'\approx\mathcal{G}$, respectively.

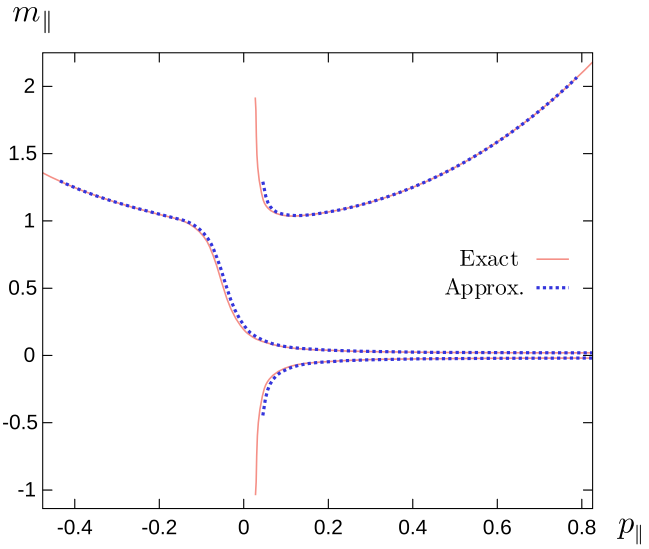

FIG. 4. (Color online) $m_\parallel(p_\parallel)$ calculated for $n_0=1$, $\omega=0.97\Omega_0$, and $\varepsilon=0.02$ (in units $m=c=q=1$): the exact expression from Ref. [5] (solid) and the approximate expression (56) (dashed).

If $n_0<1$, the points $\mathcal{F}$ and $\mathcal{G}'$ belong to the same branch of the stationary curve with $\theta_n=0$; then, $m_\parallel$ can be observed for $\tilde{\mu}<\mu_*$, where μ_* is given by

$$\mu_*^{3/2}=\left(\frac{mc^2}{\omega}\right)^{3/2}\frac{a_0}{8(1-n_0)}\sqrt{\frac{\Omega_0}{\omega}}. \tag{57}$$

On the other hand, if $n_0>1$, the points $\mathcal{F}$ and $\mathcal{G}'$ belong to different branches of the stationary curve; then, the negative-mass region is not limited at high energies (Fig. 5). In either case, NME is due to particle sticking to the resonance curve, which makes the pump wave (with the help of B_0) produce an average ponderomotive force overcompensating the perturbation F.

Finally, notice that Eq. (56) was derived under the assumption that the particle is initially in a stationary state and, hence, remains restricted to the stationary curve $J_2(J_1)$. If, however, the particle is initially displaced from this curve, it will undergo oscillations in (J_2,θ_2) space (rather than remain at a fixed location). However, the corresponding oscillation orbit will still remain centered around a stationary point mapping to the stationary curve $J_2(J_1)$. Assuming the oscillations are almost linear, the *average* $J_2(J_1)$ would be the same in this case, meaning that the above derivation for $m_\parallel$ holds also for particles that were not necessarily at a stationary state initially. Hence, away from the bifurcation points $\mathcal{F}$, corrections to Eq. (56) can result only from *large*-amplitude oscillations in (J_2,θ_2) space, i.e., at essentially relativistic transverse energies. [This conclusion also agrees with Eq. (38) of Ref. [5], from where it follows that $m_\parallel$ is not affected by the displacement from the stationary point, unless the parameter s introduced there is comparable to or larger than unity.]

IV. PARALLEL MASS INSTABILITY

At negative $m_\parallel$, particles are accelerated in the direction opposite to the external force F. Should F be the electrostatic force qE due to space-charge fluctuations in plasma, the charge will not be compensated by the induced motion of the oscillation centers but rather amplified; hence a collective instability.

The instability growth rate is found from the longitudinal wave dispersion relation. Assuming $E\sim\exp(-i\omega_0 t+ik_0 z)$, this dispersion relation may be written as [28]

$$1-\sum_s\frac{4\pi n_s q_s^2}{k_0}\int_{-\infty}^{+\infty}\frac{dp}{\omega_0-k_0 v}\frac{\partial f_s}{\partial p}=0, \tag{58}$$

where n_s is the plasma density, and $f_s(p)$ is the unperturbed distribution function of species s. Further assuming that the plasma is cold [i.e., the characteristic width of each $f_s(p)$ is much smaller than ω_0/k_0], Eq. (58) can be rewritten as

$$1+\sum_s\frac{4\pi n_s q_s^2}{\omega_0^2}\int_{-\infty}^{+\infty}dp\, v\frac{\partial f_s}{\partial p}=0. \tag{59}$$

Using that $dv=dp/m_\parallel$, one can also express Eq. (59) as

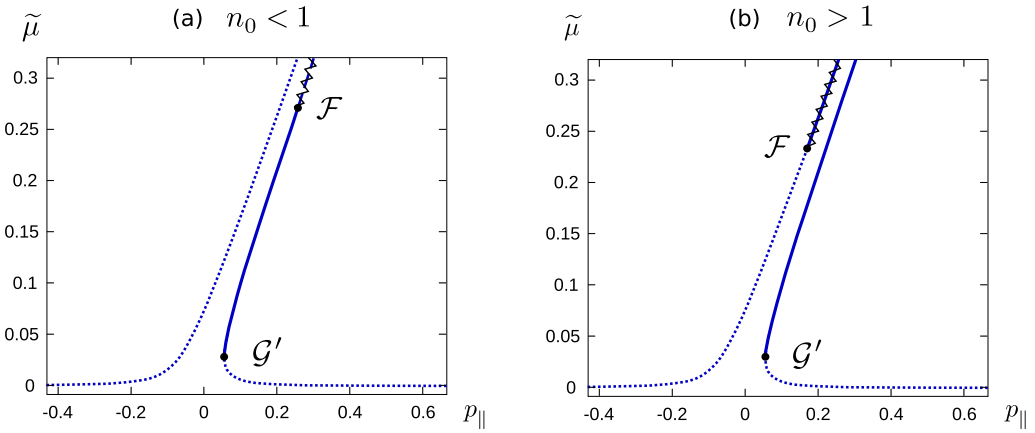

FIG. 5. (Color online) A schematic plot of the stationary curves in $(p_\parallel,\tilde{\mu})$ coordinates with the regions of positive and negative parallel mass for (a) $n_0<1$ and (b) $n_0>1$. The parts of the curves with the negative parallel mass are shown with the solid lines, while the positive-mass parts are shown with the dashed lines. The unstable parts of the plot are shown with the zig-zag lines. The points of zero and infinity $m_\parallel$ are denoted by $\mathcal{F}$ and $\mathcal{G}'$ correspondingly.

$$1 + \sum_s \frac{4\pi n_s q_s^2}{\omega_0^2} \int_{-\infty}^{+\infty} dp \left(\int^p \frac{dp_0}{m_{\|s}(p_0)} \right) \frac{\partial f_s}{\partial p} = 0. \quad (60)$$

where $m_{\|s}$ is the parallel mass of the species s. Hence, Eq. (60) can be put in the form

$$\omega_0^2 = \sum_s \frac{4\pi n_s q_s^2}{\bar{m}_{\|s}}, \quad (61)$$

where we introduced the parallel mass $\bar{m}_{\|s}$ averaged over the particle distribution,

$$\bar{m}_{\|s}^{-1} = \int_{-\infty}^{+\infty} dp\, m_{\|s}^{-1}(p) f_s(p). \quad (62)$$

Depending on $f_s(p)$, the frequency ω_0 can be either real or imaginary. In the former case, when particles with positive $m_{\|s}$ dominate, one recovers the electrostatic Langmuir oscillations, with the energy density given by $|E|^2/(8\pi)$ as usual. However, when dominant are particles with $m_{\|s} < 0$, the field E will not oscillate but rather grow exponentially. The energy that supports the instability is the quasienergy ΔK that is released when negative-mass particles leave the vicinity of the unstable equilibrium at the local maximum of $K(p)$ (Fig. 6). On the other hand, one can equivalently say that ΔK is drawn from the pump wave [which is what shapes $K(p)$], whereas negative-mass particles act as mediators connecting the pump energy reservoir with the wave field E. Correspondingly, for $n_0 < 1$, the instability can occur only when $\tilde{\mu} < \mu_*$ [Eq. (41)], which is the condition under which $m_{\|} < 0$ is possible. (For $n_0 > 1$, there is no such condition for negative-mass particles; however, at $\tilde{\mu} > \mu_*$, one of the positive-mass branches becomes unstable; see Sec. III E.)

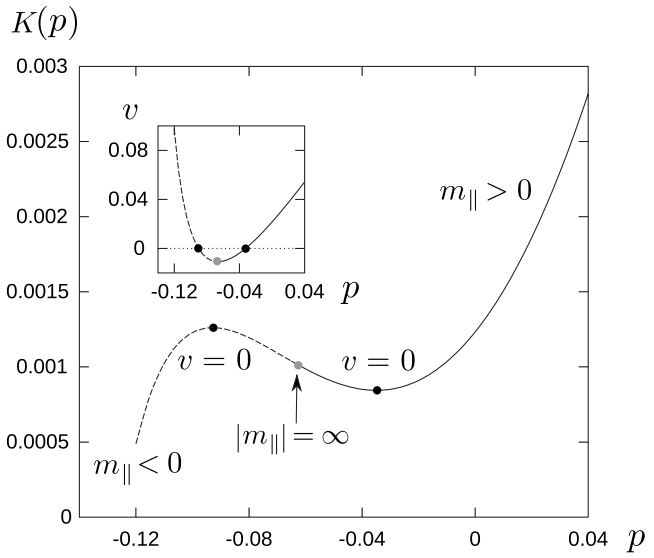

FIG. 6. The quasienergy K vs the quasimomentum p for $n=0.98$, $\omega=0.85\Omega_0$ and $\varepsilon=0.05$ (in units $m=c=q=1$), exhibiting regions of positive (solid) and negative (dashed) parallel mass $m_{\|}$. The inset also demonstrates that the velocity v is nonmonotonic as a function of p; hence, there are two distinct values of p corresponding to $v=0$ (black disks). The plot $K(p)$ shown here corresponds to the singular branches of $m_{\|}(v)$ in Fig. 5(a), merging at $|m_{\|}|=\infty$ (gray disk). The continuous branch from Fig. 5(a), corresponding to $m_{\|}$ with a fixed sign, is not shown here.

V. CONCLUSIONS

In this paper, we develop a perturbation theory for a classical particle undergoing nonlinear interaction with a wave in dielectric medium and show that the particle motion can be described in terms of an effective parallel mass which can become negative. As an example, we study a relativistic particle interacting with a circularly polarized wave propagating in a medium with refractive index n_0 close (yet not equal) to unity in the presence of a static magnetic field. We show that, when $\tilde{\mu}$ [Eq. (17)] is smaller than μ_* [Eq. (41)], there can exist up to three stationary orbits with different magnetic moments $\tilde{\mu}$, all of which are stable (centerlike). We predict that a negative parallel mass $m_{\|}$ can be realized in the vicinity of the intermediate-energy equilibrium, and report a plasma collective instability which can develop for low-frequency electrostatic waves in an oscillation-center plasma where particles with $m_{\|} < 0$ dominate.

ACKNOWLEDGMENTS

The authors thank G. M. Fraiman for stimulating and encouraging discussions. This work was supported by the NNSA under the SSAA Program through DOE Research Grant No. DE-FG52-08NA28553 and by DOE through Contract No. DEAC02-76CH03073.

[1] N. N. Bogoliubov and Y. A. Mitropolskii, *Asymptotic Methods in the Theory of Nonlinear Oscillations* (Gordon and Breach, New York, 1961), Sec. 15.
[2] L. D. Landau and E. M. Lifshitz, *Mechanics* (Pergamon Press, New York, 1960), Sec. 29.
[3] J. Fajans and L. Frièdland, Am. J. Phys. **69**, 1096 (2001).
[4] I. Y. Dodin and N. J. Fisch, Phys. Rev. E **79**, 026407 (2009).
[5] I. Y. Dodin and N. J. Fisch, Phys. Rev. E **77**, 036402 (2008).
[6] V. F. Elesin, Usp. Fiziol. Nauk **175**, 197 (2005) [Phys. Usp. **48**, 183 (2005)].
[7] A. A. Koulakov and M. E. Raikh, Phys. Rev. B **68**, 115324 (2003).
[8] K. S. Klopovsky, Zh. Tekh. Fiz. **42**, 558 (1972).
[9] C. E. Nielsen and A. M. Sessler, Rev. Sci. Instrum. **30**, 80 (1959).
[10] A. A. Kolomensky and A. N. Lebedev, Atomnaya Energiya **7**, 549 (1959) [Sov. J. At. Energy **7**, 1013 (1961)].
[11] R. W. Landau and K. Neil, Phys. Fluids **9**, 2412 (1966).
[12] Y. Y. Lau and R. J. Briggs, Phys. Fluids **14**, 967 (1971).
[13] H. S. Uhm and R. C. Davidson, Phys. Fluids **20**, 771 (1977).

[14] V. L. Bratman and A. V. Savilov, Phys. Plasmas **2**, 557 (1995).
[15] A. V. Savilov, Phys. Plasmas **4**, 2276 (1997).
[16] O. Dumbrajs, P. Nikkola, and B. Piosczyk, Int. J. Electron. **88**, 215 (2001).
[17] D. Strasser, T. Geyer, H. B. Pedersen, O. Heber, S. Goldberg, B. Amarant, A. Diner, Y. Rudich, I. Sagi, M. Rappaport, D. J. Tannor, and D. Zajfman, Phys. Rev. Lett. **89**, 283204 (2002).
[18] L. D. Shvartsman, D. A. Romanov, and J. E. Golub, Phys. Rev. A **50**, R1969 (1994).
[19] H. Mehdian, M. Esmelzadeh, and J. E. Willett, Phys. Plasmas **8**, 3776 (2001).
[20] M. Esmaeilzadeh, H. Mehdian, and J. E. Willett, Phys. Rev. E **65**, 016501 (2001).
[21] I. A. Kotel'nikov and G. V. Stupakov, Phys. Fluids B **2**, 881 (1990).
[22] A. J. Lichtenberg and M. A. Lieberman, *Regular and Chaotic Dynamics*, 2nd ed. (Springer-Verlag, New York, 1992), Sec. 2.2.
[23] G. R. Smith and A. N. Kaufman, Phys. Fluids **21**, 2230 (1978).
[24] I. Y. Dodin and N. J. Fisch, in *Frontiers in Modern Plasma Physics: 2008 ICTP International Workshop on the Frontiers of Modern Plasma Physics*, AIP Conf. Proc. No. 1061, edited by P. K. Shukla, B. Eliasson, and L. Stenflo (AIP, Melville, NY, 2008), p. 263.
[25] K. Ueno, K. Shiga, and S. Morita, *A Mathematical Gift: the Interplay between Topology, Functions, Geometry, and Algebra* (American Mathematical Society, Providence, RI, 2003), Vol. 1.
[26] A. Candel and L. Conlon, *Foliations II* (American Mathematical Society, Providence, RI, 2003).
[27] R. A. Smith, Proc. London Math. Soc. **s3-48**, 341 (1984).
[28] E. M. Lifshitz and L. P. Pitaevskii, *Physical Kinetics* (Pergamon Press, New York, 1981).
[29] C. Kittel, *Introduction to Solid State Physics*, 7th ed. (Wiley, New York, 1996), Chap. 8.
[30] In the degenerate case $n_0=1$, there always exist two stationary points for given J_1. A similar application of the Poincaré-Hopf theorem shows that they are both stable, in agreement with Ref. [5].